Reference: *Biol. Bull.* **239:** 000–000. (August 2020)

DOI: 10.1086/710126

Effects of Salinity and pH of Seawater on the Reproduction of the Sea Urchin *Paracentrotus lividus*

NUNZIA LIMATOLA[1,*], JONG TAI CHUN[2], AND LUIGIA SANTELLA[1]

[1]*Department of Research Infrastructures for Marine Biological Resources; and* [2]*Department of Biology and Evolution of Marine Organisms, Stazione Zoologica Anton Dohrn, Napoli, Italy*

Abstract. Fertilization and early development are usually the most vulnerable stages in the life of marine animals, and the biological processes during this period are highly sensitive to the environment. In nature, sea urchin gametes are shed in seawater, where they undergo external fertilization and embryonic development. In a laboratory, it is possible to follow the exact morphological and biochemical changes taking place in the fertilized eggs and the developing embryos. Thus, observation of successful fertilization and the subsequent embryonic development of sea urchin eggs can be used as a convenient biosensor to assess the quality of the marine environment. In this paper, we have examined how salinity and pH changes affect the normal fertilization process and the following development of *Paracentrotus lividus*. The results of our studies using confocal microscopy, scanning and transmission electron microscopy, and time-lapse Ca^{2+} image recording indicated that both dilution and acidification of seawater have subtle but detrimental effects on many aspects of the fertilization process. They include Ca^{2+} signaling and coordinated actin cytoskeletal changes, leading to a significantly reduced rate of successful fertilization and, eventually, to abnormal or delayed embryonic development.

Introduction

Going through fertilization, a quiescent egg is activated by a successful sperm to form a zygote—the very first diploid cell of a new living organism. Much of our knowledge on the mechanism by which a new life is generated has come from experiments on oocytes and eggs of echinoderms, such as starfish and sea urchins. Whereas only a few oocytes are released during ovulation in mammals (Shah *et al.*, 2018), sea urchins and starfish provide a large quantity of gametes that are easily accessible for experiments. Because the reproduction of these organisms relies on external fertilization, the whole process of species-specific gamete interaction, fertilization, and early development can be easily followed in the laboratory by using seawater (Meijer and Guerrier, 1984; Vacquier, 2011).

In the eggs of all animal species, a series of morphological and biochemical changes takes place at fertilization, collectively referred to as "egg activation." For example, a rapid and sustained increase in intracellular Ca^{2+} concentrations follows a precise spatiotemporal pattern to activate the egg's metabolism and to initiate embryonic development (Stricker, 1999; Parrington *et al.*, 2007; Santella *et al.*, 2012; Ramos and Wessel, 2013). In most cases, this intracellular Ca^{2+} increase can be attributed to the prompt Ca^{2+} influx as a result of sperm-induced plasma membrane depolarization and to the release from internal stores (Berridge, 1993; Runft *et al.*, 2002; Santella *et al.*, 2004; Whitaker, 2006; Santella and Chun, 2013). Concurrently, activation of Ca^{2+}-dependent Na^+/H^+ exchange pumps leads to an increase of intracellular pH, which is thought to be essential for the resumption of the cell cycle and the polymerization of actin in the sea urchin egg cortex (Johnson *et al.*, 1976; Begg and Rebhun, 1979; Swann and Whitaker, 1986; Gilbert, 2014). The increase of cytoplasmic Ca^{2+} gives rise to one of the most appreciable structural changes in the newly formed zygote, the cortical reaction (Just, 1919), which includes exocytosis of cortical granules (CG) positioned underneath the plasma membrane. The resulting extrusion of the contents of CG, such as mucopolysaccharides, hyaline proteins, and activated peroxidase and transglutaminase, leads to the thickening of a hyaline layer and to the lifting of the fertilization envelope (FE) (Hylander

* To whom correspondence should be addressed. Email: nunzia.limatola@szn.it.

Received 2 December 2019; Accepted 22 May 2020; Published online 3 August 2020.

Abbreviations: ASW, artificial seawater, filtered; CCD, charge-coupled device; CF, cortical flash; CG, cortical granule; CW, Ca^{2+} wave; FE, fertilization envelope; SW, filtered natural seawater.

and Summers, 1982; Wessel and Wong, 2009), which serves as the sole protective barrier that shields the delicate developing embryo against the external environment (Schuel, 1984).

The actin cytoskeleton of the egg surface affects gamete interactions, and the egg's cytoskeletal structure is drastically reorganized during oocyte maturation and fertilization (Santella *et al.*, 2015, 2018). In sea urchin eggs, microvilli and the acidic vesicles near the plasma membrane are known to play a crucial role in the initiation of sperm-induced Ca^{2+} signals (Vasilev *et al.*, 2019). Both structures are intimately associated with the actin meshwork. In the fertilized eggs of sea urchins and starfish, actin filaments formed on the egg surface at the site of sperm-egg interaction fill the fertilization cone (Tilney and Jaffe, 1980; Santella *et al.*, 2020). Actin bundles in the subplasmalemmal zones and fertilization cone then migrate away from the egg cortex, while the sperm inside the cytoplasm moves toward the female pronucleus (Terasaki, 1996; Puppo *et al.*, 2008; Limatola *et al.*, 2019a, b). In addition, the actin-filled microvilli elongate on the egg surface to protrude through the entire perivitelline space, thus providing mechanical support for FE elevation and accommodation of the increased membrane on the cell surface (Puppo *et al.*, 2008; Chun *et al.*, 2010). All of these changes in the structural organization and function of the actin cytoskeleton in the egg are thought to be essential for adequate fertilization events: sperm-egg interaction, proper intracellular Ca^{2+} signaling, efficient CG exocytosis, FE elevation, and the entry of only one sperm (Puppo *et al.*, 2008; Chun and Santella, 2009; Chun *et al.*, 2013, 2014; Limatola *et al.*, 2015, 2019a, b). Treadmilling of actin filaments also influences Ca^{2+} buffering (Lange, 1999), and the polymerization status of the actin cytoskeleton influences the activities of intracellular calcium channels and the enzymes involved in Ca^{2+} signaling pathways (Bose and Thomas, 2009; Chun *et al.*, 2013; Vasilev *et al.*, 2018).

In the past decades, the growing concern for global warming has been extended to consequential changes in the marine environment. Mainly as a result of industrialized anthropogenic activities, the level of carbon dioxide (CO_2) in the atmosphere has been continually increasing at an alarming rate (Solomon *et al.*, 2009). When dissolved in water, the increased CO_2 would produce excessive bicarbonate, leading to the decrease of seawater pH (Caldeira *et al.*, 2003; Feely *et al.*, 2004; Orr *et al.*, 2005; Huntington, 2006). Thus, the emerging view is that accelerated climate changes may cause not only rising seawater temperature but also unexpected problems of seawater acidification and salinity changes. These are due to the drastic alterations of rainfall, such as El Niño, which are predicted to worsen in the coming decades (IPCC, 2013) and to affect the salinity gradient in the transition zone between rivers and oceans (Allen and Pechenik, 2010; Cloern *et al.*, 2017). Considering this worrying scenario and the potential risk for health-related environmental issues, it is worth investigating the effect of these changes on the reproduction of marine organisms. Indeed, as a benthic marine invertebrate, *Paracentrotus lividus* (Lamarck, 1816) and its planktonic larvae are known to be continually subjected to multiple stress factors resulting from global climate changes (Byrne and Przeslawski, 2013).

Several early studies found a reduction in fertilization rate in response to water acidification, warming, or salinity variations. However, their analyses were mostly focused either on how the marine environmental changes alter sperm quality, density, and motility (Havenhand *et al.*, 2008; Schlegel *et al.*, 2015; Campbell *et al.*, 2016) or on how the altered size and quantity of eggs produced at spawning affect cleavages and embryonic development (Allen and Pechenik, 2010; Carballeira *et al.*, 2011; Moulin *et al.*, 2011; Foo and Byrne, 2017); few additional studies paid attention to the general quality of the eggs (Podolsky, 2002; Ciapa and Philippe, 2013; Foo and Byrne, 2017; Parker *et al.*, 2017). Given that, we tested in this study the hypothesis that acidification and salinity changes of seawater directly affected the morphology and physiology of individual eggs of sea urchin. To this end, we altered the pH or salinity of seawater and examined how these simulated changes affect the structure and dynamics of actin filaments of the egg cortex and the pattern of Ca^{2+} signaling at fertilization, as well as subsequent embryonic development.

Materials and Methods

Gamete collection and modifications of seawater parameters

Paracentrotus lividus (Lamarck, 1816) was collected from the Gulf of Naples during its breeding season (from October to May) and kept in circulating seawater (16 °C). Female animals were stimulated by intracoelomic injection of 0.5 mol L^{-1} KCl, and the eggs were collected in a small dish filled with natural seawater filtered with a membrane of 0.2 μm pore size (Nalgene vacuum filtration system, Rochester, NY), which is referred to as seawater (SW) in this study. Sperm were collected by pipetting on the male animal's body surface, and the dry sperm were stored at 4 °C. Fertilization in SW was performed with a final sperm concentration of 1.84×10^6 cells per mL. To visualize egg-incorporated spermatozoa, sperm nuclei were stained with 5 μmol L^{-1} Hoechst-33342 (Sigma-Aldrich, St. Louis, MO) about 30 seconds before fertilization. Sperm incorporation was observed five minutes after egg insemination by using a cooled CCD (charge-coupled device) camera (MicroMax, Princeton Instruments, Trenton, NJ) mounted on a Zeiss Axiovert 200 microscope with a Plan Neofluar 40×/0.75 objective with a UV laser (Oberkochen, Germany). Because only sperm, and not the eggs, were stained with the DNA marker Hoechst-33342, the background fluorescence was low enough for us to discern the weak but punctate signals coming from the individual sperm by changing focus and scanning the whole visual depth of the living eggs.

The Hoechst-33342 in the media of sperm occasionally visualized the female pronucleus of the zygotes, but it was easily distinguishable from the signals of sperm DNA for the different sizes. The decrease of SW salinity was achieved by adding distilled water until the desired dilution percentage was reached, and the salinity was increased by adding NaCl to SW to effect an increment of 275 mmol L^{-1} extra NaCl in the medium (as described in Just, 1939, p. 192). The lowering of the SW pH was obtained by adding HCl immediately before the experiment. In order to decrease Na^+ concentrations, filtered artificial seawater (ASW, 575 mmol L^{-1} NaCl, 10 mmol L^{-1} KCl, 10 mmol L^{-1} $CaCl_2$, 55 mmol L^{-1} $MgSO_4$, 2 mmol L^{-1} $NaHCO_3$, pH 8.1) was mixed with Na^+-free ASW (575 mmol L^{-1} choline chloride, 10 mmol L^{-1} KCl, 10 mmol L^{-1} $CaCl_2$, 55 mmol L^{-1} $MgSO_4$, 2 mmol L^{-1} $NaHCO_3$, pH 8.1), as previously described (Limatola *et al.*, 2019b). The exact ionic composition of seawater of the Mediterranean is variable, like any other seawater (Sanfilippo *et al.*, 2016); and Mediterranean seawater is known to be slightly saltier than ocean seawater. The basic parameters of the various conditions of seawater that we used for our experiment are summarized in Table A1.

Microinjection, confocal microscopy, and Ca^{2+} imaging

Microinjection of individual eggs was performed with an air pressure transjector (Eppendorf FemtoJet, Hamburg, Germany) as previously described (Chun *et al.*, 2014). To visualize F-actin in living intact eggs, 10 μmol L^{-1} AlexaFluor568-phalloidin (Molecular Probes, Eugene, OR) was microinjected; and the eggs were monitored with a CrEST X-Light spinning disk confocal microscope (Crisel Elettrooptical Systems and Technology, Rome, Italy) or with a Leica TCS SP8 X confocal laser scanning microscope, equipped with a white light laser and hybrid detectors (Leica Microsystem, Wetzlar, Germany). In this low concentration, Alexa-phalloidin does not appear to interfere with the biological processes in the eggs but visualizes F-actin in echinoderm egg cortex as faithfully as LifeAct-GFP (green fluorescent protein), as judged by the images that were quite comparable (Vasilev *et al.*, 2018). To visualize Ca^{2+} in fertilized eggs, 500 μmol L^{-1} Calcium Green 488 conjugated with 10 kDa dextran was mixed with 35 μmol L^{-1} Rhodamine Red (Molecular Probes) in the injection buffer (10 mmol L^{-1} HEPES, 0.1 mol L^{-1} potassium aspartate, pH 7.0) and microinjected before insemination. The fluorescence images of cytosolic Ca^{2+} and the bright-field view images were captured with a cooled CCD camera (MicroMax, Princeton Instruments) mounted on a Zeiss Axiovert 135TV microscope with a Plan-Neofluar 40×/0.75 objective at about 3-second intervals, and the data were analyzed with MetaMorph (Universal Imaging, Bedford Hills, NY). The Ca^{2+} signal at a given time point was quantified following the formula $F_{rel} = [(F - F_0)/F_0]$, where F represents the average fluorescence level of the entire egg and F_0 represents baseline fluorescence. Thus, F_{rel} was defined as a relative fluorescence unit (RFU) for plotting Ca^{2+} trajectories. To visualize the site of instantaneous Ca^{2+} release, the incremental change of the Ca^{2+} level at each moment at time point t was analyzed by applying the formula $F_{inst} = [(F_t - F_{t-1})/F_{t-1}]$. To compensate batch-to-batch variability of Ca^{2+} signals, the peak amplitudes of the cortical flash (CF) and Ca^{2+} wave (CW) of each egg were normalized with the averages of the corresponding values in the control eggs from the same batch (taken as 100%).

Statistical analyses

The numerical MetaMorph data were compiled and analyzed with Excel of Microsoft Office 2010. The average and variation of the data are reported as mean ± standard deviation (SD) in all cases in this article. One-way ANOVA and *post hoc* tests were performed by using Prism 8.0 (GraphPad, San Diego, CA), and P-values smaller than 0.05 were considered statistically significant.

Transmission electron microscopy (TEM)

Paracentrotus lividus eggs were fixed in SW containing 0.5% glutaraldehyde (pH 8.1) for 1 hour at room temperature and post-fixed with 1% osmium tetroxide for an additional 1 hour. Specimens were dehydrated in increasing concentrations of ethanol and were embedded in Epon 812, then stained with UAR-EMS (Uranyl Acetate Replacement Stain, Electron Microscope Sciences, Hatfield, PA) for 30 minutes and 0.3% lead citrate for 30 seconds. The specimens were examined under a transmission electron microscope (Zeiss LEO 912 AB).

Scanning electron microscopy (SEM)

Sea urchin eggs were fixed in filtered seawater containing 0.5% glutaraldehyde (pH 8.1) for 1 hour at room temperature and post-fixed with 1% osmium tetroxide for an additional 1 hour. Specimens were dehydrated in increasing concentrations of ethanol, and subsequent critical-point drying was performed (Leica EM CP300). Samples were then coated with a thin layer of metal, using a Leica ACE200 sputter-coater, and were observed with a JEOL 6700F scanning electron microscope (Akishima, Tokyo, Japan).

Results

Embryonic development of Paracentrotus lividus *perturbed by environmental change not attributable to multiple sperm incorporation*

In line with previous studies (Reuter *et al.*, 2011; Ross *et al.*, 2011; Byrne *et al.*, 2013), alterations of several seawater parameters led to inhibition of the first cleavages and delayed embryonic development. This was already evident when the eggs were inseminated in the 75% SW (Fig. 1A). Likewise,

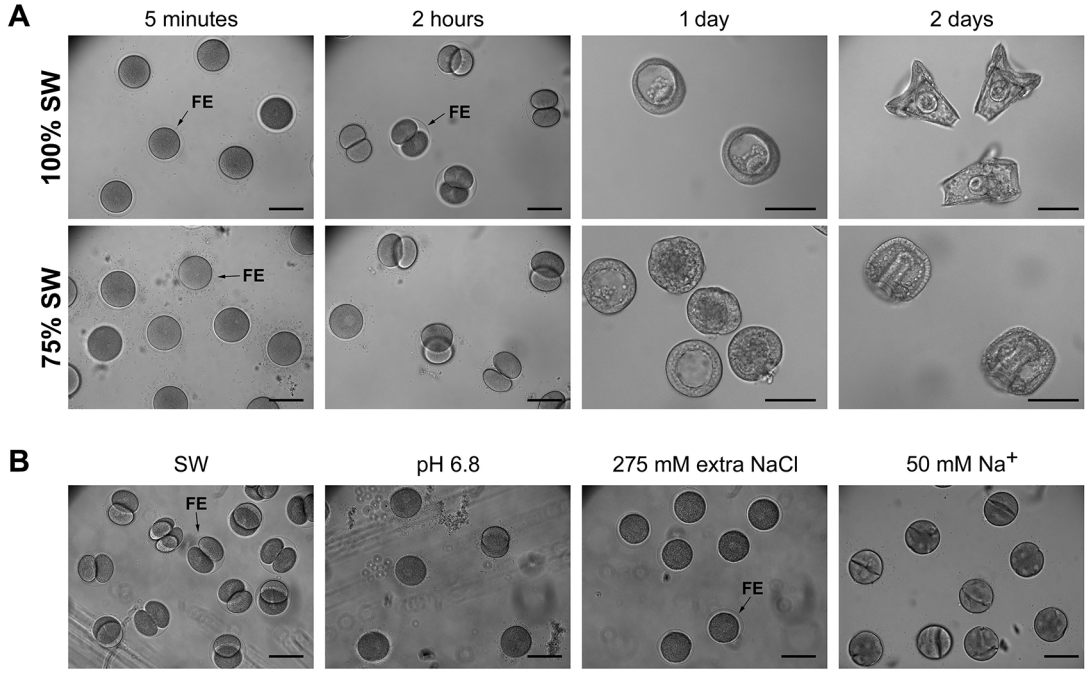

Figure 1. Alterations of seawater pH and salinity delay embryonic development or inhibit the cleavage of *Paracentrotus lividus*. Bright-field view images of the early embryos after egg insemination in various conditions. (A) Effects of dilution (75%) of natural and filtered seawater (SW). (B) Embryos 2 hours after fertilization in normal SW, acidic SW at pH 6.8, hypertonic seawater (275 mmol L^{-1} extra NaCl), or in artificial seawater with 50 mmol L^{-1} Na^{+}. The number of fertilized eggs examined in each condition was 100. The experiments were repeated at least two times. FE, fertilization envelope. Scale bars = 100 μm.

the eggs fertilized in SW with low pH (6.8) or hypertonic conditions all exhibited drastically delayed or failed cleavage by two hours after fertilization, whereas eggs fertilized in ASW with low sodium underwent apparent failure at cytokinesis (Fig. 1B; see also Limatola *et al.*, 2019b). The percentage of the eggs undergoing normal development on schedule in each condition is summarized in Table 1. To test whether this abnormal pattern of embryonic development was due to polyspermic fertilization, we incubated the eggs for 15 minutes in seawater, with changes of various abiotic factors, and counted the egg-incorporated sperm 5 minutes after insemination. In this context, it should be noted that fertilization is a multistep process that involves chemotaxis, gamete binding and fusion, ion flux, Ca^{2+} increases, sperm entry, and the union of haploid male and female pronuclei. In this study, the entry of fluorescence-labeled sperm into the egg cytoplasm is referred to as "incorporation." As shown in Figure 2, the sperm failed to enter the egg in extremely low salinity SW (40%) in all cases ($n = 20$), although sperm-egg binding and a compromised Ca^{2+} signal were observed (Fig. 3). Thus, it appears that beyond a certain extent of seawater dilution, entry of the sperm into an egg does not take place, at least in this species. Indeed, exposure of the eggs to diluted SW (75%) or hypertonic SW (275 mmol L^{-1} extra NaCl) did not make significant differences to the number of egg-incorporated sperm (always monospermy) or affect the extent of FE elevation (>95% eggs showed full elevation); but in the latter case, the zygotes failed to undergo normal cleavages (Fig. 1). In addition, several steps of fertilization were more susceptible to a lower pH (6.8), because the elevation of the FE occurred only in some area of the egg membrane (partial elevation, 20% of the cases) or on the entire surface but with a much reduced and non-equidistant lifting (thin elevation, 80% of the cases, Fig. 2B). These results imply that the morpho-functional properties of the cortex (*e.g.*, capability of CG exocytosis) are more severely affected by the seawater pH in the given experimental conditions. Nonetheless, nearly all of

Table 1

Percentages of embryos following normal and abnormal development

	2 hours		1 day		2 days	
	Normal	Abnormal	Normal	Abnormal	Normal	Abnormal
SW	98	2	96	4	96	4
75% SW	85	15	25	75	0	100
pH 6.8	16	84				
275 mmol L^{-1} extra NaCl	0	100				
50 mmol L^{-1} Na^{+}	0	100				

SW, natural and filtered seawater.

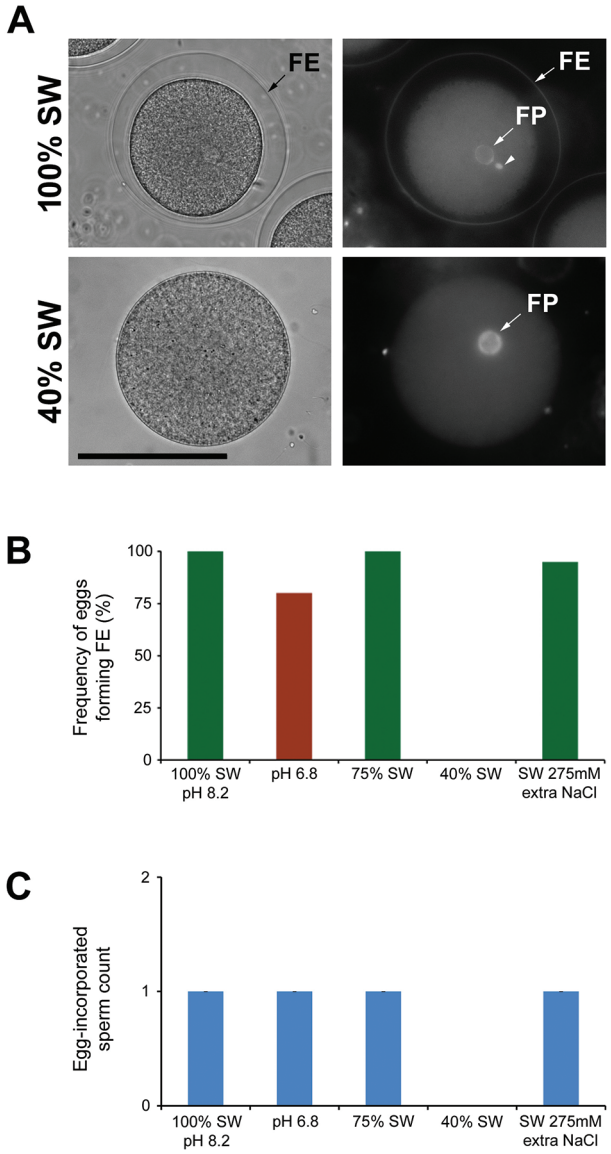

Figure 2. Seawater salinity and pH changes affect embryonic development without inducing polyspermy. *Paracentrotus lividus* eggs were preincubated for 15 minutes and fertilized in 100% natural and filtered seawater (SW) or 75% SW. (A) Sperm entry visualized by Hoechst-33342 in living eggs fertilized in 100% SW or 40% SW. Note the fertilization envelope (FE) and the single sperm incorporated in the eggs fertilized in 100% SW (white arrowhead), which were not present in the eggs fertilized in 40% SW. Female pronucleus (FP) visualized by Hoechst-33342. Scale bar = 100 μm. (B, C) Graphic summary of the effects of pH and salinity on fertilization. The number of eggs examined for each condition was 20 (total $n = 100$). (B) About 5 minutes after insemination, the elevation of the fertilization envelope (FE) was examined in the bright-field view; the frequency of eggs (%) showing full elevation of FE is presented in green bars. The eggs showing partial or thin elevation are presented with red histograms. (C) Average number of egg-incorporated sperm was calculated from the pooled data at the given condition and is presented with blue histograms.

the eggs fertilized in low pH or moderately diluted seawater were predominantly monospermic (Fig. 2C), even though they tended either to fail to undergo proper cleavage by two hours post-fertilization or to delay the embryonic development (Fig. 1).

Effect of altered seawater salinity and pH on Ca^{2+} responses in the fertilized eggs of sea urchin

To test whether the egg's physiological response to the fertilizing sperm is affected by altered seawater salinity and pH, we recorded the dynamics of Ca^{2+} increase during the fertilization process by the use of calcium dyes. We exposed sea urchin eggs for 15 minutes to various conditions of seawater as specified in *Materials and Methods* and fertilized them with spermatozoa collected in SW. Once added to the eggs, the sperm shared the same media with the eggs, that is, seawater with varied pH, salinity, and so on. In the given conditions, we first assessed the instant effect of pH and salinity changes on the sperms' motility or their effectiveness in interacting with the egg by measuring the time interval between insemination and the onset of the intracellular CW, which occurred in all of the experimental conditions. We found that sperm added to the eggs suspended in hypertonic SW (275 mmol L^{-1} extra NaCl) failed to reach the surface of the egg, suggesting that sperm motility is sharply sensitive to hypertonic salinity. Unlike eggs inseminated in other seawater conditions, eggs exposed to hypertonic seawater had to be moved back to SW to allow fertilization. Except for the hypertonic seawater, we found that the sperm's efficacy in inducing a CW in the egg was not affected much by the altered pH and salinity conditions tested. Indeed, the time lag between insemination and the onset of a CW in these eggs was not significantly different from that of the eggs fertilized in SW, because the pairwise comparison indicated that the time lag in SW was not significantly different from any of the values in other conditions (SW, 62.1 ± 30.8 s, $n = 55$; 40% SW, 105.3 ± 44.3 s, $n = 40$; seawater pH 6.8, 54.1 ± 33.7 s, $n = 16$, one-way ANOVA, $P < 0.05$; Tukey honest significant different [HSD] test: SW *vs.* each condition, none significant).

As to the Ca^{2+} response in the eggs of *P. lividus* fertilized in SW, the earliest detectable Ca^{2+} signal at fertilization is the CF (Fig. 3A), a synchronous Ca^{2+} influx through the entire surface of the egg induced by opening of voltage-gated ion channels due to plasma membrane depolarization. The CF is followed by an intracellular CW that propagates on the egg surface from the sperm-egg interaction site toward the opposite pole (Vasilev *et al.*, 2019). When the eggs were preincubated in 40% SW (15 min), they took up water by osmotic pressure and increased in volume (Fig. 3A). Upon fertilization in 40% SW, CF was not detectable in most eggs (39 of 54), while it was always present in the eggs fertilized in normal seawater ($n = 55$, see Fig. 3A). Furthermore, even if the peak amplitude of the CW was not affected much by dilution of the seawater (40% SW, see brown curves in Fig. 3A), the FE elevation did not take place (Fig. 2A). By contrast, when the eggs were incubated in SW containing 275 mmol

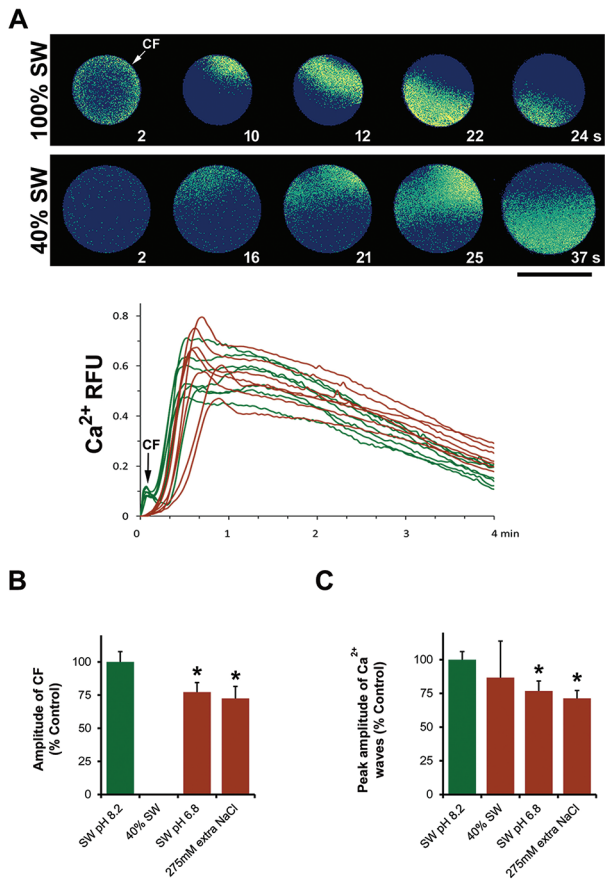

Figure 3. Effects of seawater pH and salinity alterations on the intracellular Ca^{2+} increase in sea urchin eggs at fertilization. *Paracentrotus lividus* eggs microinjected with calcium dyes were incubated in natural and filtered seawater (SW) with the specific salinity or pH for 15 minutes and were fertilized. The changes in the intracellular Ca^{2+} levels following fertilization were monitored with a CCD (charge-coupled device) camera. (A) Pseudocolored relative fluorescence images represent the sites of momentary Ca^{2+} increases at the indicated time points (seconds). Note the increment of the egg diameter due to the osmotic pressure in 40% SW. CF, cortical flash. In the graph, the Ca^{2+} trajectories show the relative Ca^{2+} levels in the control (green curves) and 40% SW (brown curves) from one batch. The time frame immediately before the first detectable Ca^{2+} signal captured by the CCD camera was set to $t = 0$. RFU, relative fluorescence units. Scale bar = 100 μm. (B, C) Comparison of the Ca^{2+} responses in the eggs fertilized in various conditions. (B) Amplitudes of the cortical flash. (C) Peak amplitude of the Ca^{2+} waves. Error bars represent standard deviation. $^*P < 0.001$ in comparison with the control (SW, pH 8.2).

L^{-1} extra NaCl, the residence in this medium brought about the exit of water from the eggs, as evidenced by their shrinkage (83 μm in diameter in 275 mmol L^{-1} extra NaCl *vs.* 90 μm in SW). When the eggs were fertilized in normal SW after preincubation in high-salinity SW or at pH 6.8, the amplitudes of both the CF and CW were significantly reduced (Fig. 3B, C). Conversely, the CW propagated more slowly in the eggs fertilized in diluted seawater (40% SW), as judged by the time required for the CW to traverse the egg (eggs in 40% SW, 38.5 ± 7.27 s, $n = 54$; eggs in SW, 19.47 ± 1.6 s, $n = 55$, $P < 0.0001$). This nearly twofold difference in the planar speed of the CW far exceeded the difference in the egg diameters caused by egg swelling (115 μm in 40% SW *vs.* 90 μm in SW). However, the swelling increased the surface area and the volume of the eggs by 63% and 109%, respectively. Hence, the components propagating the CW in the cytoplasmic matrix may have become sparser or lost their integrity—and thereby may have become less efficient in spreading the wave—in addition to the increase of the physical distance the wave has to travel in the swollen egg. This perturbation of egg Ca^{2+} dynamics is also likely to arise from the structural changes of the egg cortex that compromised the fertilization response (Vasilev *et al.*, 2012, 2019; Chun *et al.*, 2013, 2014; Limatola *et al.*, 2015, 2019a, b).

Effect of altered seawater salinity and low pH on actin dynamics at fertilization

To test the idea that the compromised sperm-induced Ca^{2+} signaling, CG exocytosis, sperm incorporation, and embryonic development in the eggs fertilized in seawater with altered salinity and pH are linked to the alteration of the cortical structures and actin dynamics, we examined the actin cytoskeleton and the ultrastructure of these eggs. For the sake of efficient illustration of their effects on cytoskeletal morphology and egg ultrastructure, which is often difficult to demonstrate in milder conditions, we focused instead on some drastic conditions (Figs. 4, 5). For the visualization of actin filaments in living cells, Alexa-phalloidin was microinjected into the eggs, which were then transferred to media of various conditions: SW, 40% SW, SW at pH 6.8, or hypertonic SW (275 mmol L^{-1} extra NaCl). After 15 minutes, the sperm solution was added to the same medium, except for the eggs exposed to hypertonic SW, which were transferred back to SW. In SW (Fig. 4A, first row, $n = 13$), by 10 minutes after the sperm-egg interaction, the actin filaments were arranged perpendicularly to the egg plasma membrane. These filaments then migrated progressively toward the center of the egg. In hypotonic seawater, the actin cytoskeleton of the unfertilized eggs lost its proper structure and functionality at fertilization. Indeed, when the eggs were preincubated and fertilized in 40% SW, the perpendicular fibers and their orderly centripetal migration were not observed; but there was a massive time-dependent depolymerization of the filaments in the cytoplasm (Fig. 4A, second row, $n = 6$), which might in part explain the failure of sperm entry at fertilization. Moreover, eggs incubated in pH 6.8 ($n = 9$) or hypertonic seawater ($n = 9$) for 15 minutes exhibited selective hyperpolymerization of actin in the subplasmalemmal zone. When fertilized, the actin dynamics in these eggs were again compromised in comparison with the control eggs in SW (Fig. 5). When examined with TEM and SEM, unfertilized eggs exposed to low-salinity seawater exhibited heavily compromised ultrastructure of the egg cytoplasm and loss of the orderly disposition of CG in the cortex

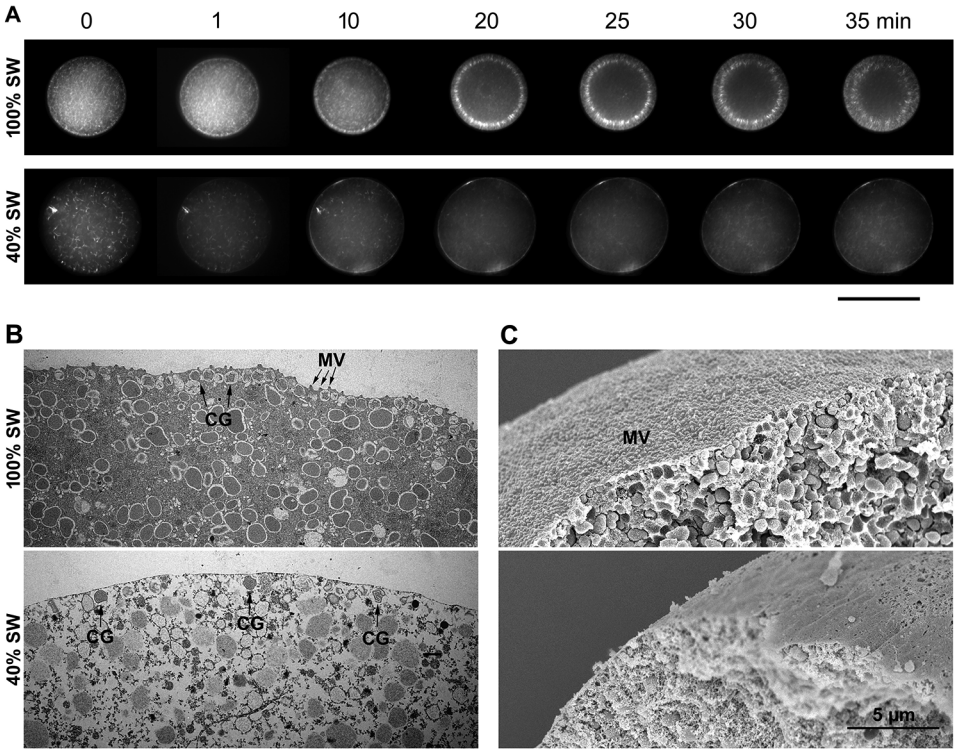

Figure 4. Low salinity of seawater heavily perturbs the actin dynamics at fertilization and egg ultrastructure. (A) Spinning disk confocal microscope images of actin cytoskeleton in *Paracentrotus lividus* eggs microinjected with the fluorescent probe for F-actin (Alexa-phalloidin) and preincubated in 100% natural and filtered seawater (SW) or 40% SW for 15 minutes and inseminated. For each condition, the moment immediately before sperm addition was taken as $t = 0$, and the time-lapse images of the actin cytoskeleton were obtained with confocal microscopy at the equatorial plane. Scale bar = 100 μm. Note the centripetal translocation of the actin bundles from the subplasmalemmal regions, visible only in eggs fertilized in 100% SW and not in diluted SW. (B) Ultrastructure of the egg cortex and cytoplasm of an unfertilized egg viewed by transmission electron microscopy (TEM) after 15 minutes of incubation in 100% SW or 40% SW. Note the disappearance of microvilli (MV) on the egg surface in the eggs exposed to 40% SW as compared to the control and the heavily compromised egg cytoplasm ultrastructure. CG, cortical granules. (C) Scanning electron microscopy (SEM) images of fractured sea urchin eggs to view the cytoplasm and the egg cortex and surface after 15 minutes of incubation in 100% SW or 40% SW, showing the dramatic alteration of the structural organization of the egg cytoplasm due to water entry.

(Fig. 4B, C). Also, the profile of the plasma membrane displayed the shortening or loss of microvilli, with the myriad F-actin-filled protrusions evident on the surface of the eggs in SW (Fig. 4B, C). Taken together, these results suggest that the changes of the structure and function of the egg actin cytoskeleton in the media with altered salinity and acidity contribute to the compromised physiological responses of the egg at the time of fertilization, egg activation, and subsequent cleavages.

Discussion

With increasing awareness of recent climate changes, one of the key concerns has been how they may influence marine life and the ecosystem. In this communication, we demonstrated that alteration of seawater salinity and pH has fundamental impacts on the morphology and physiology of individual eggs of sea urchins. Our data showed that intricate mechanisms controlling the actin cytoskeleton of the egg surface, gamete interaction, and intracellular Ca^{2+} increases in fertilized eggs go astray in the demonstrable cases of seawater acidification (pH 6.8) and dilution (75% or 40%).

In early studies, the effect of environmental changes on the success of fertilization was merely estimated by the so-called fertilization curve approach (Reuter *et al.*, 2011; Sewell *et al.*, 2014), which showed that the influence of sperm density on successful fertilization was shifted by the environmental changes. It is noteworthy, however, that the judgment of successful fertilization was often based on the percentages of the resulting embryos undergoing normal cleavages. In this context, it bears emphasis that aberrant cleavage is not necessarily caused by the formation of multiple sperm asters related to polyspermy but can result from perturbation of the cortical integrity of the egg, which, in optimum conditions, incorporates a single sperm (Just, 1939; Puppo *et al.*, 2008; Vasilev *et al.*, 2012; Chun *et al.*, 2014; Limatola *et al.*, 2019a, b). Here, we

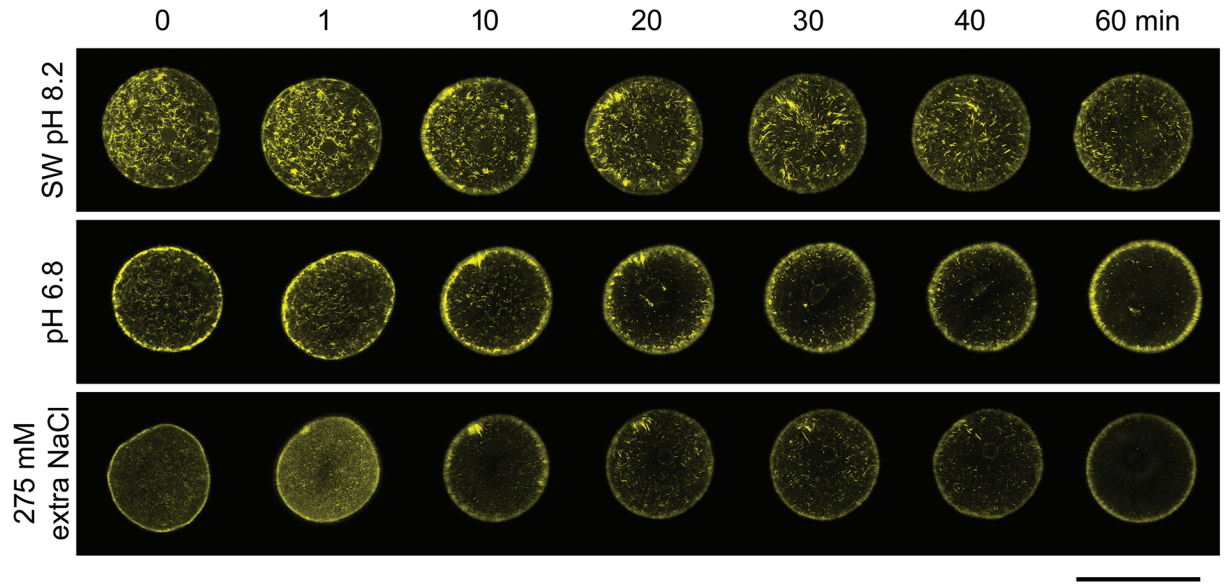

Figure 5. Changes of the actin cytoskeleton of the eggs exposed to seawater with low pH or high salinity. *Paracentrotus lividus* eggs were microinjected with Alexa-phalloidin and preincubated for 15 minutes in acidic (pH 6.8) or hypertonic (275 mL extra NaCl) seawater. For the latter case, eggs were transferred back to natural and filtered seawater (SW). The eggs were then fertilized with sperm, and the changes of the actin cytoskeleton were monitored by laser confocal scanning microscopy. For comparison, eggs incubated in normal SW (pH 8.2) were included in the parallel experiment. Represented results from nine different eggs were shown for each condition. Scale bar = 100 μm.

corroborate that the abnormal embryonic development may arise from monospermic zygotes and that the integrity of the egg cortical structure and its changes after insemination may be the primary parameters for successful fertilization and development, as noted earlier (Just, 1939). Indeed, the first cleavage was blocked in the majority of the conditions being tested (Fig. 1); but this phenomenon was not due to polyspermy, because most eggs incorporated only one sperm (Fig. 2).

The cortical actin cytoskeleton of starfish and sea urchin eggs actively participates in the cascade of events regulating the fertilization processes, such as interaction with sperm, Ca^{2+} signals, egg activation, and sperm entry into the egg (Santella and Chun, 2011; Santella *et al.*, 2015, 2018). The establishment of contact between the acrosomal filament (which contains F-actin) of the sperm and the actin filaments in the egg's cytoplasm provides strong anchorage for the sperm to enter the egg (Puppo *et al.*, 2008; Santella *et al.*, 2014, 2020; Chun *et al.*, 2018; Limatola *et al.*, 2019a). When the structure of the actin cytoskeleton is altered with pharmacological agents, the sperm incorporation in starfish and sea urchin eggs was severely affected (Puppo *et al.*, 2008; Vasilev *et al.*, 2012; Chun *et al.*, 2014). This idea was further supported by the finding that in the eggs incubated in 40% SW, the sperm failed to enter the egg due to the dramatic alteration of the structural organization of the actin filaments in the egg cortex (Fig. 4A), although it was still able to transduce a Ca^{2+} signal (albeit altered) following its interaction with the egg surface. In 40% SW, despite the lack of CF, the sperm induced a CW with amplitude similar to that of the eggs fertilized in 100% SW (Fig. 3A). Nevertheless, upon insemination, and at variance with the prevailing view, these eggs with compromised cortical F-actin and cytoplasmic structure failed to undergo Ca^{2+}-dependent CG exocytosis and FE elevation, as previously shown (Santella *et al.*, 2015).

As aforementioned, in virtually all animal species, the interaction between the gametes gives rise to a signal transduction cascade, in which Ca^{2+} plays a pivotal role in successful egg activation (Berridge, 1993; Parrington *et al.*, 2007; Santella *et al.*, 2012; Costache *et al.*, 2014; Stricker, 2014). While the modification of salinity, pH, or ion concentrations of seawater is eventually expected to influence the intracellular environment, acidification of seawater did not change the egg lipid contents in oysters (Parker *et al.*, 2017). However, it was reported that the internal pH of sea urchin eggs could be affected by the external environment (Ciapa and Philippe, 2013). Because cytosolic pH affects the synthesis, phosphorylation, and activation of proteins of eggs (Johnson and Epel, 1976), it is not surprising that the acidification of seawater (pH 6.8) caused changes of the egg actin cytoskeleton (Fig. 5) and reduced the amplitudes of the CF and CW (Fig. 3). Similar to the eggs in acidic seawater (pH 6.8), eggs in hypertonic seawater displayed comparable alterations of actin cytoskeletal structure and the diminution of CF and CW amplitudes (Figs. 3, 5). As to the effects on Ca^{2+} signaling, perhaps the most remarkable observation in our study is that CF was abolished in most of the eggs fertilized in 40%

SW (Fig. 3A, B). Because CF represents Ca^{2+} influx triggered by plasma membrane depolarization, this result may arise from the changes of the electrical properties of the plasma membrane in 40% SW. Besides the fact that the Ca^{2+} concentration in the media is also diluted to 40% of the normal level, the given experimental condition in our study involving egg swelling and severe retraction of microvilli on the plasma membrane does not rule out the possibilities that (i) the resting potential of the eggs in 40% SW was somehow depolarized to the level that no longer enables CF to occur or (ii) the voltage-gated Ca^{2+} channels were underrepresented in the plasma membrane with the exhaustive retraction of microvilli. In line with this, it is worth pointing out that the amplitude of CF altered by various drugs and physical conditions in sea urchin eggs is often paralleled by the changes of microvilli shape or density on the egg surface (Vasilev *et al.*, 2019; Santella *et al.*, 2020).

According to recent studies of starfish and sea urchin eggs, the onset, magnitude, and kinetics of the sperm-induced CF and CW are largely dependent on actin structure and dynamics in the egg cortex (Nusco *et al.*, 2006; Puppo *et al.*, 2008; Chun *et al.*, 2010, 2014; Vasilev *et al.*, 2012, 2019; Limatola *et al.*, 2019a, b). In sea urchin eggs, the amplitude of CF can be repressed by jasplakinolide, an actin drug that stabilizes F-actin (Chun *et al.*, 2014). Another drug stabilizing F-actin, phalloidin, however, enhances its amplitude. Conversely, the agents depolymerizing actin (latrunculin A and cytochalasin B) rather prolong the duration of CF without changing its amplitude. These actin drugs also affect the CW pattern (Chun *et al.*, 2014). Thus, the onset and other features of CF and CW dynamics are thought to be affected by the state of F-actin, including the ones present in microvilli, and possibly by the cortical CG and vesicles being connected to the plasma membrane by actin networks, as was proposed previously (Vasilev *et al.*, 2019). In support of the idea, in the overmaturing eggs of starfish whose microvilli and cortical actin cytoskeleton underwent meiotic stage-dependent restructuring, the amplitude of the CF and CW displayed fluctuations (Limatola *et al.*, 2019a). Thus, the lack of a CF and the apparent decrease in CW speed in the eggs fertilized in 40% SW (Fig. 3A) should also be viewed in light of the facts that nearly all microvilli are retracted from the egg surface and that the egg cytoplasm is severely perturbed where CG and vesicles are embedded. Recently, our findings in starfish and sea urchin eggs, underscoring the relationship between the cortical actin network, Ca^{2+} response, and CG exocytosis during egg activation, have been extended to other animal species (Lee *et al.*, 2016; Vogt *et al.*, 2019; York-Andersen *et al.*, 2019).

In conclusion, it appears that normal reorganization of the egg cortical actin cytoskeleton is the essential prerequisite to ensure proper sperm-egg interaction, a normal Ca^{2+} response, successful fertilization, and normal embryonic development in echinoderms. Our results demonstrate that many aspects of fertilization and embryonic development are heavily influenced by the pH and salinity of seawater. Considering the alarming rate of global climate change and its impact on the oceans, the presence of these stress factors might highly influence the distribution, growth, and physiology of marine species, which may eventually affect the marine ecosystems (Byrne and Przeslawski, 2013; IPCC, 2013).

Acknowledgments

We are grateful to D. Caramiello for the careful maintenance of sea urchin *Paracentrotus lividus* and the measurement of physical seawater parameters and to G. Gragnaniello, F. Iamunno R. Graziano, and G. Lanzotti for their technical assistance at the Advanced Microscopy Center of the Stazione Zoologica Anton Dohrn (SZN) in Naples, Italy. This research was supported by the SZN. NL has been financially supported by an SZN postdoctoral fellowship. We thank the anonymous reviewers for their careful reading of the manuscript and for helpful comments and suggestions.

Literature Cited

Allen, J. D., and J. A. Pechenik. 2010. Understanding the effects of low salinity on fertilization success and early development in the sand dollar *Echinarachnius parma*. *Biol. Bull.* **218:** 189–199.

Begg, D. A., and L. I. Rebhun. 1979. pH regulates the polymerization of actin in the sea urchin egg cortex. *J. Cell Biol.* **83:** 241–248.

Berridge, M. J. 1993. Cell signaling: a tale of two messengers. *Nature* **365:** 388–389.

Bose, D. D., and D. W. Thomas. 2009. The actin cytoskeleton differentially regulates NG115-401L cell ryanodine receptor and inositol 1,4,5-trisphosphate receptor induced calcium signaling pathways. *Biochem. Biophys. Res. Commun.* **379:** 594–599.

Byrne, M., and R. Przeslawski. 2013. Multistressor impacts of warming and acidification of the ocean on marine invertebrates' life histories. *Integr. Comp. Biol.* **53:** 582–596.

Byrne, M., M. A. Ho, L. Koleits, C. Price, C. K. King, P. Virtue, B. Tilbrook, and M. Lamare. 2013. Vulnerability of the calcifying larval stage of the Antarctic sea urchin *Sterechinus neumayeri* to near-future ocean acidification and warming. *Glob. Change Biol.* **19:** 2264–2275.

Caldeira, K., and M. E. Wickett. 2003. Anthropogenic carbon and ocean pH. *Nature* **425:** 365.

Campbell, A. L., D. R. Levitan, D. J. Hosken, and C. Lewis. 2016. Ocean acidification changes the male fitness landscape. *Sci. Rep.* **6:** 31250.

Carballeira, C., L. Martín-Díaz, and T. A. Delvalls. 2011. Influence of salinity on fertilization and larval development toxicity tests with two species of sea urchin. *Mar. Environ. Res.* **72:** 196–203.

Chun, J. T., and L. Santella. 2009. Roles of the actin-binding proteins in intracellular Ca^{2+} signalling. *Acta Physiol.* **195:** 61–70.

Chun, J. T., A. Puppo, F. Vasilev, G. Gragnaniello, E. Garante, and L. Santella. 2010. The biphasic increase of PIP2 in the fertilized eggs of starfish: new roles in actin polymerization and Ca^{2+} signaling. *PLoS One* **5:** e14100.

Chun, J. T., F. Vasilev, and L. Santella. 2013. Antibody against the actin-binding protein depactin attenuates Ca^{2+} signaling in starfish eggs. *Biochem. Biophys. Res. Commun.* **441:** 301–307.

Chun, J. T., N. Limatola, F. Vasilev, and L. Santella. 2014. Early events of fertilization in sea urchin eggs are sensitive to actin-binding organic molecules. *Biochem. Biophys. Res. Commun.* **450:** 1166–1174.

Chun, J. T., F. Vasilev, N. Limatola, and L. Santella. 2018. Fertilization in starfish and sea urchin: roles of actin. *Results Probl. Cell Differ.* **65:** 33–47.

Ciapa, B., and L. Philippe. 2013. Intracellular and extracellular pH and Ca are bound to control mitosis in the early sea urchin embryo *via* ERK and MPF activities. *PLoS One* **8:** e66113.

Cloern, J. E., A. D. Jassby, T. S. Schraga, E. Nejad, and C. Martin. 2017. Ecosystem variability along the estuarine salinity gradient: examples from long-term study of San Francisco Bay. *Limnol. Oceanogr.* **62:** S272–S291.

Costache, V., A. McDougall, and R. Dumollard. 2014. Cell cycle arrest and activation of development in marine invertebrate deuterostomes. *Biochem. Biophys. Res. Commun.* **450:** 1175–1181.

Feely, R. A., C. L. Sabine, K. Lee, W. Berelson, J. Kleypas, V. J. Fabry, and F. J. Millero. 2004. Impact of anthropogenic CO_2 on the $CaCO_3$ system in the oceans. *Science* **305:** 362–366.

Foo, S. A., and M. Byrne. 2017. Marine gametes in a changing ocean: impacts of climate change stressors on fecundity and the egg. *Mar. Environ. Res.* **128:** 12–24.

Gilbert, S. F. 2014. Activation of egg metabolism in sea urchins. Pp. 134–139 in *Developmental Biology*, 10th edition. Sinauer Associates, Sunderland, MA.

Havenhand, J. N., F. R. Buttler, M. Thorndyke, and J. E. Williamson. 2008. Near-future levels of ocean acidification reduce fertilization success in a sea urchin. *Curr. Biol.* **18:** R651–R652.

Huntington, T. G. 2006. Evidence for intensification of the global water cycle: review and synthesis. *J. Hydrol.* **319:** 83–95.

Hylander, B. L., and R. G. Summers. 1982. An ultrastructural immunocytochemical localization of hyalin in the sea urchin egg. *Dev. Biol.* **93:** 368–380.

IPCC (Intergovernmental Panel on Climate Change). 2013. Summary for policymakers. Pp. 119–1310 in *Climate Change 2013: The Physical Science Basis. Contribution of Working Group I to the Fifth Assessment Report of the Intergovernmental Panel on Climate Change*, T. F. Stocker, D. Qin, G. K. Plattner, M. Tignor, S. K. Allen, J. Boschung, A. Nauels, Y. Xia, V. Bex, and P. M. Midgley, eds. Cambridge University Press, Cambridge.

Johnson, J. D., and D. Epel. 1976. Intracellular pH and activation of sea urchin eggs after fertilisation. *Nature* **262:** 661–664.

Just, E. E. 1919. The fertilization reaction in *Echinarachnius parma*. I. Cortical response of the egg to insemination. *Biol. Bull.* **36:** 1–10.

Just, E. E. 1939. *The Biology of the Cell Surface*. P. Blakiston's Son, Philadelphia.

Lange, K. 1999. Microvillar Ca^{++} signaling: a new view of an old problem. *J. Cell Physiol.* **180:** 19–34.

Lee, H. C., S. Y. Yoon, K. Lykke-Hartmann, R. A. Fissore, and I. Carvacho. 2016. TRPV3 channels mediate Ca^{2+} influx induced by 2-APB in mouse eggs. *Cell Calcium* **59:** 21–31.

Limatola, N., J. T. Chun, K. Kyozuka, and L. Santella. 2015. Novel Ca^{2+} increases in the maturing oocytes of starfish during the germinal vesicle breakdown. *Cell Calcium* **58:** 500–510.

Limatola, N., F. Vasilev, J. T. Chun, and L. Santella. 2019a. Altered actin cytoskeleton in ageing eggs of starfish affects fertilization process. *Exp. Cell Res.* **381:** 179–190.

Limatola, N., F. Vasilev, J. T. Chun, and L. Santella. 2019b. The sodium-mediated fast electrical depolarization does not prevent polyspermic fertilization in *Paracentrotus lividus* eggs. *Zygote* **27:** 241–249.

Meijer, L., and P. Guerrier. 1984. Maturation and fertilization in starfish oocytes. *Int. Rev. Cytol.* **86:** 129–196.

Moulin, L., A. I. Catarino, T. Claessens, and P. Dubois. 2011. Effects of seawater acidification on early development of the intertidal sea urchin *Paracentrotus lividus* (Lamarck 1816). *Mar. Pollut. Bull.* **62:** 48–54.

Nusco, G. A., J. T. Chun, E. Ercolano, D. Lim, G. Gragnaniello, K. Kyozuka, and L. Santella. 2006. Modulation of calcium signaling by the actin-binding protein cofilin. *Biochem. Biophys. Res. Commun.* **348:** 109–114.

Orr, J. C., V. J. Fabry, O. Aumont, L. Bopp, S. C. Doney, R. A. Feely, A. Gnanadesikan, N. Gruber, A. Ishida, F. Joos *et al.* 2005. Anthropogenic ocean acidification over the twenty-first century and its impact on calcifying organisms. *Nature* **437:** 681–686.

Parker, L. M., W. A. O'Connor, M. Byrne, R. A. Coleman, P. Virtue, M. Dove, M. Gibbs, L. Spohr, E. Scanes, and P. M. Ross. 2017. Adult exposure to ocean acidification is maladaptive for larvae of the Sydney rock oyster *Saccostrea glomerata* in the presence of multiple stressors. *Biol. Lett.* 20160798.

Parrington, J., L. C. Davis, A. Galione, and G. Wessel. 2007. Flipping the switch: how a sperm activates the egg at fertilization. *Dev. Dyn.* **236:** 2027–2038.

Podolsky, R. D. 2002. Fertilization ecology of egg coats: physical *versus* chemical contributions to fertilization success of free-spawned egg. *J. Exp. Biol.* **205:** 1657–1668.

Puppo, A., J. T. Chun, G. Gragnaniello, E. Garante, and L. Santella. 2008. Alteration of the cortical actin cytoskeleton deregulates Ca^{2+} signaling, monospermic fertilization, and sperm entry. *PLoS One* **3:** e3588.

Ramos, I., and G. M. Wessel. 2013. Calcium pathway machinery at fertilization in echinoderms. *Cell Calcium* **53:** 16–23.

Reuter, K. E., K. E Lotterhos, R. N. Crim, C. A. Thompson, and C. D. G. Harley. 2011. Elevated pCO_2 increases sperm limitation and risk of polyspermy in the red sea urchin *Strongylocentrotus franciscanus*. *Glob. Change Biol.* **17:** 163–171.

Ross, P. M., L. Parker, W. A. O'Connor, and E. A. Bailey. 2011. The impact of ocean acidification on reproduction, early development and settlement of marine organisms. *Water* **3:** 1005–1030.

Runft, L. L., L. A. Jaffe, and L. M. Mehlmann. 2002. Egg activation at fertilization: where it all begins. *Dev. Biol.* **245:** 237–254.

Sanfilippo, M., G. Capillo, N. Spanò, and A. Manganaro. 2016. Evaluation of water variables in no-take zone of Ustica Marine Protected Area (southern Tyrrhenian Sea). *Braz. Arch. Biol. Technol.* **59:** e16160330.

Santella, L., and J. T. Chun. 2011. Actin, more than just a housekeeping protein at the scene of fertilization. *Sci. China Life Sci.* **54:** 733–743.

Santella, L., and J. T. Chun. 2013. Calcium signaling by cyclic ADP-ribose and NAADP. Pp. 331–337 in *Encyclopedia of Biological Chemistry*, W. J. Lennarz and M. D. Lane, eds. Academic Press, Waltham, MA.

Santella, L., D. Lim, and F. Moccia. 2004. Calcium and fertilization: the beginning of life. *Trends Biochem. Sci.* **29:** 400–408.

Santella, L., F. Vasilev, and J. T. Chun. 2012. Fertilization in echinoderms. *Biochem. Biophys. Res. Commun.* **425:** 588–594.

Santella, L., N. Limatola, and J. T. Chun. 2014. Actin cytoskeleton and fertilization in starfish eggs. Pp. 141–155 in *Sexual Reproduction in Animals and Plants*, H. Sawada, N. Inoue, and M. Iwano, eds. Springer, Tokyo.

Santella, L., N. Limatola, and J. T. Chun. 2015. Calcium and actin in the saga of awakening oocytes. *Biochem. Biophys. Res. Commun.* **460:** 104–113.

Santella, L., N. Limatola, F. Vasilev, and J. T. Chun. 2018. Maturation and fertilization of echinoderm eggs: role of actin cytoskeleton dynamics. *Biochem. Biophys. Res. Commun.* **506:** 361–371.

Santella, L., N. Limatola, and J. T. Chun. 2020. The cellular and molecular aspects of oocyte maturation and fertilization: a perspective from the actin cytoskeleton. *Zool. Lett.* **6:** 5.

Schlegel, P., M. T. Binet, J. N. Havenhand, C. J. Doyle, and J. E. Williamson. 2015. Ocean acidification impacts on sperm mitochondrial membrane potential bring sperm swimming behaviour near its tipping point. *J. Exp. Biol.* **218:** 1084–1090.

Schuel, H. 1984. The prevention of polyspermic fertilization in sea urchins. *Biol. Bull.* **167:** 271–309.

Sewell, M. A., R. B. Millar, P. C. Yu, L. Kapsenberg, and G. E. Hofmann. 2014. Ocean acidification and fertilization in the Antarctic sea urchin *Sterechinus neumayeri*: the importance of polyspermy. *Environ. Sci. Technol.* **48:** 713–722.

Shah, J. S., R. Sabouni, K. C. Cayton Vaught, C. M. Owen, D. F. Albertini, and J. H. Segars. 2018. Biomechanics and mechanical signaling in the ovary: a systematic review. *J. Assist. Reprod. Genet.* **3:** 1135–1148.

Solomon, S., G. K. Plattner, R. Knutti, and P. Friedlingstein. 2009. Irreversible climate change due to carbon dioxide emissions. *Proc. Natl. Acad. Sci. U.S.A.* **106:** 1704–1709.

Stricker, S. A. 1999. Comparative biology of calcium signaling during fertilization and egg activation in animals. *Dev. Biol.* **211:** 157–176.

Stricker, S. A. 2014. Calcium signaling and endoplasmic reticulum dynamics during fertilization in marine protostome worms belonging to the phylum Nemertea. *Biochem. Biophys. Res. Commun.* **450:** 1182–1187.

Swann, K., and M. Whitaker. 1986. The part played by inositol trisphosphate and calcium in the propagation of the fertilization wave in sea urchin eggs. *J. Cell Biol.* **103:** 2333–2342.

Terasaki, M. 1996. Actin filament translocations in sea urchin eggs. *Cell Motil. Cytoskelet.* **34:** 48–56.

Tilney, L. G., and L. A. Jaffe. 1980. Actin, microvilli, and the fertilization cone of sea urchin eggs. *J. Biol. Chem.* **87:** 771–782.

Vacquier, V. D. 2011. Laboratory on sea urchin fertilization. *Mol. Reprod. Dev.* **78:** 553–564.

Vasilev, F., J. T. Chun, G. Gragnaniello, E. Garante, and L. Santella. 2012. Effects of ionomycin on egg activation and early development in starfish. *PLoS One* **7:** e39231.

Vasilev, F., N. Limatola, D. R. Park, U. H. Kim, L. Santella, and J. T. Chun. 2018. Disassembly of subplasmalemmal actin filaments induces cytosolic Ca^{2+} increases in *Astropecten aranciacus* eggs. *Cell Physiol. Biochem.* **48:** 2011–2034.

Vasilev, F., N. Limatola, J. T. Chun, and L. Santella. 2019. Contributions of suboolemmal acidic vesicles and microvilli to the intracellular Ca^{2+} increase in the sea urchin eggs at fertilization. *Int. J. Biol. Sci.* **15:** 757–775.

Vogt, E. J., K. Tokuhiro, M. Guo, R. Dale, G. Yang, S. W. Shin, M. J. Movilla, H. Shroff, and J. Dean. 2019. Anchoring cortical granules in the cortex ensures trafficking to the plasma membrane for post-fertilization exocytosis. *Nat. Commun.* **10:** 2926.

Wessel, G. M., and J. L. Wong. 2009. Cell surface changes in the egg at fertilization. *Mol. Reprod. Dev.* **76:** 942–953.

Whitaker, M. 2006. Calcium at fertilization and in early development. *Physiol. Rev.* **86:** 25–88.

York-Andersen, A. H., G. Hu, B. W. Wood, M. F. Wolfner, and T. T. Weil. 2019. A calcium-mediated actin redistribution at egg activation in *Drosophila*. *Mol. Reprod. Dev.* **87:** 293–304.

Appendix

Table A1

Basic parameters of the various conditions of seawater being used in the study

	Acidity (pH)	Salinity (PSU)	Electric conductivity (mS cm^{-1})
SW	8.2	37.8	46
40% SW	8.2	15.8	22.2
75% SW	8.2	24.1	31.5
pH 6.8	6.8	37.8	45.9
275 mmol L^{-1} extra NaCl	8.2	47.4	56.6
ASW	8.1	41	52.8
50 m NaCl ASW	8.1	33.5	42.3

ASW, artificial seawater; PSU, practical salinity unit; SW, seawater, natural and filtered.